

Optimal margin and edge-enhanced intensity maps in the presence of motion and uncertainty

Timothy C Y Chan¹, John N Tsitsiklis² and Thomas Bortfeld³

¹ Mechanical and Industrial Engineering, University of Toronto, Toronto, ON M5S3G8, CANADA

² Laboratory for Information and Decision Systems, Massachusetts Institute of Technology, Cambridge, MA 02139, USA

³ Department of Radiation Oncology, Massachusetts General Hospital and Harvard Medical School, Boston, MA 02114, USA

E-mail: tcychan@mie.utoronto.ca, jnt@mit.edu and tbortfeld@partners.org

November 23, 2009 - Revised

Abstract. In radiation therapy, intensity maps involving margins have long been used to counteract the effects of dose blurring arising from motion. More recently, intensity maps with increased intensity near the edge of the tumour (edge-enhancements) have been studied to evaluate their ability to offset similar effects that affect tumour coverage. In this paper, we present a mathematical methodology to derive margin and edge-enhanced intensity maps that aim to provide tumour coverage while delivering minimum total dose. We show that if the tumour is at most about twice as large as the standard deviation of the blurring distribution, the optimal intensity map is a pure scaling increase of the static intensity map without any margins or edge-enhancements. Otherwise, if the tumour size is roughly twice (or more) the standard deviation of motion, then margins and edge-enhancements are preferred, and we present formulae to calculate the exact dimensions of these intensity maps. Furthermore, we extend our analysis to include scenarios where the parameters of the motion distribution are not known with certainty, but rather can take any value in some range. In these cases, we derive a similar threshold to determine the structure of an optimal margin intensity map.

Submitted to: *Phys. Med. Biol.*

1. Introduction

The use of margins has long been studied and implemented in practice as a technique to mitigate the effects of any phenomenon that may degrade treatment quality in radiation therapy. Margins have been employed to combat everything from setup uncertainty to motion to imaging artifacts (International Commission on Radiation Units and Measurements 1999). Their ubiquity in treatment planning is a testament to their effectiveness, relative ease of implementation, but also lack of dominant substitutes. Due to the inherent trade-off in using a margin (increased likelihood of tumour coverage versus increased dose to the healthy tissue), the question of minimizing the size of the margin while maintaining its efficacy is of great interest. While many empirical studies have focused on applying margins to clinical cases and proposed methods to reduce the size of the margin, others have taken a more theoretical approach to analyzing margins and produced rules of thumb to govern their design (Balter et al. 1995, Goitein 1985, Ekberg et al. 1998, Roach et al. 1994, van Herk et al. 2000). In particular, the seminal work presented in (van Herk et al. 2000) generated a significant leap in the understanding and design of margins. One of the goals of this paper will be to introduce a new method of determining optimal margins in the face of (known) motion, and produce rules of thumb that tell us *when* to use a margin and exactly *what* size it should be. We will focus on parameters specific to an individual such as tumour size and standard deviation of motion in order to deterministically derive tailored margins. We will characterize optimal margin intensity maps (i.e., the derived margin width) in the presence of motion with a known distribution. Through our analysis, we will also address the question of when it may be advantageous to simply increase the intensity of the static beam without a margin expansion. Our effort to derive optimal margins is similar to calculating ideal spatial dose distributions (Sir et al. 2006), though our mathematical formulations are different.

The concept of an “edge-enhanced” intensity map was first introduced and studied in the context of mitigating the effects of beam penumbra (Biggs and Shipley 1986, Lind et al. 1993, Mohan et al. 1996, Dirkx et al. 1997, Brugmans et al. 1999, Sharpe et al. 2000). More recently, edge-enhanced intensity maps have been used to combat the effects of motion when the distribution is known (Lof et al. 1995, Unkelbach and Oelfke 2004, Trofimov et al. 2005) and motion when the distribution is unknown (Chan et al. 2006, Bortfeld et al. 2008). Edge-enhanced intensity maps are characterized by areas of high intensity at the edge of the tumour, coupled with lower, uniform intensity in the interior of the tumour. In the face of motion uncertainty, edge-enhancements were optimized to be a specific combination of intensity-modulation and intensity-homogeneity that allowed the intensity map to effectively balance the competing requirements of dose minimization and tumour coverage (Bortfeld et al. 2008). Though these edge-enhanced intensity maps have become more prevalent in the literature through empirical studies, there has been no analytical characterization of their “optimal” size. Therefore, the second aim of this paper is to provide the first such

characterization (i.e., specify the derived height and width of the edge-enhancements), along the lines of the analysis we will conduct for optimal margin sizes and known motion.

The third topic we will address is the topic of robustness and motion uncertainty. It is important to understand the effects of motion when we do not have a complete characterization of its distribution since wrongly assuming the reproducibility of a specific motion trajectory can cause serious dosimetric errors (Sheng et al. 2006). This is what we refer to as “motion uncertainty”. It is well understood that motion may have a large impact on treatment quality (Bortfeld et al. 2002, Goitein 2004, Webb 2006), but much analysis and experimentation often hinges on the knowledge of said motion (Zhang et al. 2004, Trofimov et al. 2005, Unkelbach and Oelfke 2004). If the motion is perfectly reproducible, periodic or known with certainty, we do not consider it a source of uncertainty. That is not to say it does not have the potential to seriously degrade the quality of a treatment. We simply separate into two situations the cases where we assume a known motion distribution and its associated parameters, and those cases where the exact motion distribution is not completely specified a priori (i.e., motion uncertainty). Therefore, the third aim of this paper will be to extend our optimal margin analysis from the realm of known motion to motion uncertainty. More precisely, we will explore the sensitivity of solutions to motion uncertainty and demonstrate that optimized margins can easily be derived to mitigate this uncertainty.

The rest of the paper will be organized as follows. In Section 2, we describe the problem geometries to be analyzed, the structural characteristics of margin and edge-enhanced intensity maps, the type of motion and motion uncertainty under consideration, and the mathematical formulations used to derive the optimal intensity maps. In Section 3, we will address the following three questions:

- (i) What is the analytical structure of an optimal margin intensity map in the presence of motion with a known distribution (also, when is a positive margin better than simply increasing the intensity, with no margin expansion)?
- (ii) How does the analytical structure of a margin intensity map change to compensate for motion with an unknown distribution (also, how sensitive are treatment plans to motion uncertainty)?
- (iii) What is the analytical structure of an optimal edge-enhanced intensity map in the presence of motion with a known distribution (also, when are edge-enhancements better than margins or simply increasing the intensity)?

Last, we synthesize our findings in Section 4. Portions of this work are derived from (Chan 2007), where the mathematical proofs that are omitted from this paper may be found.

2. Methods

In this paper, we focus on one-dimensional geometries, though an extension to three dimensions is summarized in Appendix C and described in full detail in (Chan 2007). Initially, the one-dimensional tumour is subjected to motion following a one-dimensional Gaussian distribution with known mean and standard deviation. The first objective is to design static intensity maps (restricted in structure to margin and edge-enhanced intensity maps) that simultaneously ensure tumour coverage, while minimizing the total dose delivered. Then, we extend our analysis to consider motion uncertainty, where the mean and standard deviation of the Gaussian are not known with certainty, but lie in intervals representing a range of possible parameter values. As a result, the structure of the optimal static intensity maps are revised to take into account the parameter uncertainty.

In the next few subsections, we specify the geometries considered, introduce mathematical notation that will be used throughout the remainder of this paper, and present the optimization formulations that will be used to derive both kinds of optimal intensity maps.

2.1. Problem setup

We consider a one-dimensional tumour of length t , centered at the origin, that requires one unit of dose (uniformly) throughout. This geometry is used primarily to build intuition and motivate further analyses on this topic. The tumour is subjected to Gaussian motion with mean μ and standard deviation σ . The motivation for this motion model is multi-fold. First, motion that is not Gaussian by nature (e.g., breathing motion) has been observed to converge to a Gaussian distribution if baseline corrections are not made (Engelsman et al. 2005). Second, random setup uncertainty is a type of motion that has been shown to follow a Gaussian distribution (Schewe et al. 1996). Third, extensions of this analysis to multiple sources of uncertainty will be aided by assuming a Gaussian distribution since many errors with arbitrary distributions will converge to a Gaussian. In fact, one could interpret the two Gaussian parameters as incorporating two different types of uncertainty: σ for random errors and μ for systematic errors. Fourth, a practical consideration is that a Gaussian has attractive analytical properties that facilitate the subsequent analysis. While we have focused on one-dimensional Gaussian motion, extensions to multiple dimensions (especially with radial symmetry) are logical follow-ons. We will use ϕ to denote the standard normal (Gaussian) probability density function (PDF) and Φ to denote its cumulative distribution function (CDF):

$$\phi(x) = \frac{1}{\sqrt{2\pi}}e^{-x^2/2}, \quad \Phi(x) = \int_{-\infty}^x \phi(z)dz. \quad (1)$$

In the case of motion uncertainty, we assume that the uncertain mean, $\tilde{\mu}$, lies in the interval $[\underline{\mu}, \bar{\mu}]$ and similarly, $\tilde{\sigma}$ lies in the interval $[\underline{\sigma}, \bar{\sigma}]$. While the true mean and

standard deviation can be anywhere in their respective intervals (and therefore unknown a priori), the endpoints of these intervals are assumed to be known. Therefore, the determination of intensity maps that ensure tumour coverage need to account for all possible means and standard deviations in these intervals. It is important to make the distinction between “motion” versus “motion uncertainty” here. In the first case, the mean and standard deviation of the Gaussian are known a priori, so while there is motion present, it does not necessarily imply uncertainty (only that we must appropriately account for this motion). On the other hand, motion uncertainty implies there is some specific aspect of the motion that is unknown to us and only can be learned upon treatment (or retrospectively). We may assume the motion belongs to a certain family of distributions and that its parameters are within some general bounds, but the exact values of these parameters are unknown during the treatment design phase. Therefore, not only must we account for the motion, we must also account for all of the different possible motion distributions that may be realized for different realizations of the underlying parameters.

Finally, we ignore the effects of geometric and radiation penumbrae. While this assumption is mainly for the sake of analytical convenience, it is not particularly restrictive. First, the dosimetric effects of geometric penumbra tend to be negligible and dominated by those of the radiation penumbra (Thomas 1994). Furthermore, both effects can be modeled using Gaussian distributions (Ulmer and Harder 1995). Since the sum of Gaussian random variables is Gaussian (Bertsekas and Tsitsiklis 2002), we may assume that the Gaussian motion distribution used in this paper also accounts for the effects of these other penumbrae; this is another benefit of modeling the motion as a Gaussian. Even though we only focus on motion, the results presented in this paper can be interpreted as including multiple penumbrae by simply decomposing the Gaussian standard deviation into its component parts: separate terms for motion, geometric penumbra, and radiation penumbra. Therefore, references to the standard deviation of motion can be thought of as the standard deviation of the blurring distribution (that might be comprised of all three penumbra effects).

Now, let us define the two families of intensity maps to which we will restrict our search of optimal solutions: margins and edge-enhancements.

2.2. Margin intensity maps

In the absence of motion, the optimal intensity map is a “square wave” with a height of one, length of t , and centered on the tumour – that is, it replicates the shape of the tumour exactly. In the presence of motion, the dose delivered is blurred (Bortfeld et al. 2004), which mathematically corresponds to a convolution of the motion probability density function (PDF) with the static delivered intensity map (Lujan et al. 1999, Engelsman et al. 2005, Bortfeld et al. 2002). In our setup, when the square wave intensity map is convolved with a Gaussian, the resulting function has a height strictly less than one (due to the fact that the Gaussian integrates to one and

is positive on the entire real line), which means that the tumour is being underdosed. There are two options to improve tumour coverage. One possibility is simply to deliver more than one unit of dose in the initial intensity map. The other possibility is to add a positive, isotropic margin around the tumour. Note that in the second case, a positive scaling (increase) of the intensity will still be required to achieve coverage (again, due to the convolution with the Gaussian). Our goal is to find a margin intensity map that minimizes the total dose delivered while ensuring that sufficient dose is delivered to the tumour even after the intensity map is convolved with a Gaussian PDF. As part of this analysis, we will determine precisely when an optimal intensity map should have no margin (and simply scale the initial intensity map of length t) versus when an optimal intensity map should have a positive margin. Figure 1 illustrates the dose blurring, margin, and intensity scaling concepts.

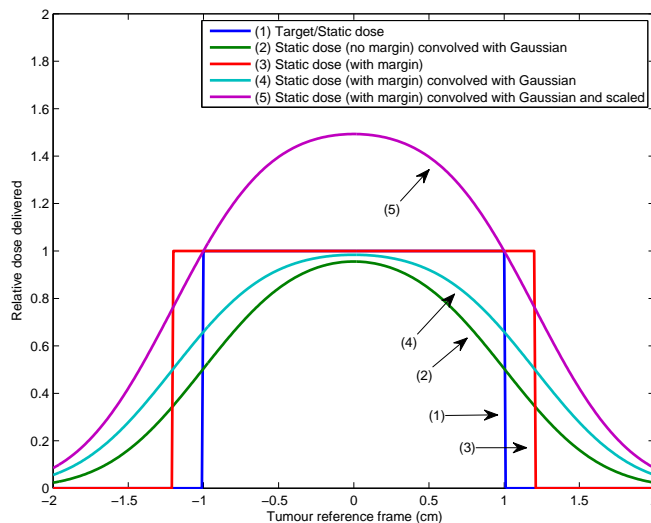


Figure 1. Dose delivered using a margin plus intensity scaling.

Let us now precisely define some notation and the concept of a margin intensity map. A *margin intensity map* has an isotropic margin of width $m \geq 0$ around an intensity map with the same width as the tumour, resulting in an intensity map of width of $t + 2m$. Formally, we define a static intensity map with a margin of size m , centered at the origin, to be

$$\delta_m(x) = \begin{cases} 1, & x \in [-t/2 - m, t/2 + m], \\ 0, & \text{otherwise.} \end{cases} \quad (2)$$

Furthermore, we define $d_m(y; \mu, \sigma)$ to be the dose delivered to point y , when a static intensity map with margin size m is convolved with a Gaussian PDF with mean μ and standard deviation σ . Hence,

$$d_m(y; \mu, \sigma) = \Phi\left(\frac{y + t/2 + m - \mu}{\sigma}\right) - \Phi\left(\frac{y - t/2 - m - \mu}{\sigma}\right). \quad (3)$$

Intuitively, an optimal intensity map should be centered on the tumour, so without loss of generality, we assume that $\mu = 0$ so that the tumour, the intensity map, and the delivered dose profile are all centered at the origin.

With a margin of size m , the total dose delivered before scaling the intensity map is $t + 2m$. Let γ be a variable that defines the multiplicative factor by which the total intensity map is scaled. We then have the following mathematical formulation of the problem of finding an intensity map that ensures tumour coverage at lowest total dosage:

$$\begin{aligned} & \underset{m, \gamma}{\text{minimize}} && \gamma(t + 2m) \\ & \text{subject to} && \gamma d_m(y; 0, \sigma) \geq 1, \quad \forall y \in [-t/2, t/2], \\ & && m, \gamma \geq 0. \end{aligned} \tag{4}$$

For a given margin size m , we define γ_m^* to be the optimal (minimal) scaling factor. Note that γ should be as small as possible while ensuring the constraint in (4) is satisfied; this implies that at some point y in the tumour, the constraint should hold with equality. Given the symmetry and unimodal natures of both the tumour and the Gaussian, the lowest point of dose in the tumour after convolution will be at its edge (at $y = t/2$ or $y = -t/2$). As long as the edge of the tumour receives enough dose, the entire tumour will receive enough dose. By inserting $y = t/2$ or $y = -t/2$ into the constraint in (4) and changing it to an equality, we get the following equation for γ_m^* :

$$\gamma_m^* = \frac{1}{\Phi\left(\frac{t+m}{\sigma}\right) - \Phi\left(\frac{-m}{\sigma}\right)} = \frac{1}{\Phi\left(\frac{m}{\sigma}\right) - \Phi\left(\frac{-t-m}{\sigma}\right)}. \tag{5}$$

Using the equation for γ_m^* , formulation (4) can be simplified to:

$$\begin{aligned} & \underset{m}{\text{minimize}} && f(m) \\ & \text{subject to} && m \geq 0, \end{aligned} \tag{6}$$

where

$$f(m) := \gamma_m^*(t + 2m) = \frac{t + 2m}{\Phi\left(\frac{t+m}{\sigma}\right) - \Phi\left(\frac{-m}{\sigma}\right)}. \tag{7}$$

The function $f(m)$ describes the total dose delivered by an intensity map that ensures tumour coverage, as a function of m . Our goal is to derive an optimal margin size (optimal value for m , from which the optimal scaling factor γ^* will follow) for any problem instance (a given t and σ). Section 3.1 summarizes the results of our analysis.

2.3. Margins under uncertainty

In the case of motion uncertainty, we have an uncertain mean, $\tilde{\mu}$, and standard deviation $\tilde{\sigma}$, that may lie anywhere in the range $[\underline{\mu}, \bar{\mu}]$ and $[\underline{\sigma}, \bar{\sigma}]$, respectively. These intervals characterize the range of possible realizations of the uncertain parameters. As in formulation (4), our objective is to minimize the total dose delivered while ensuring tumour coverage. However, with an uncertain mean and standard deviation, we wish to ensure tumour coverage *under any possible realization of $\tilde{\mu}$ and $\tilde{\sigma}$* . An intensity map

that guarantees tumour coverage while minimizing total dose in this situation will be called an optimal “robust” solution.

The quantity $\tilde{\mu}$ can be dealt with in a straightforward manner. The requirement of tumour coverage for all $\tilde{\mu} \in [\underline{\mu}, \bar{\mu}]$ is equivalent to requiring tumour coverage for a tumour that is $\bar{\mu} - \underline{\mu}$ units larger than t . Thus, we center the beam at $(\bar{\mu} + \underline{\mu})/2$, shift the origin of our coordinate system to this location, and define the “effective tumour” as the interval $[-t/2 - (\bar{\mu} - \underline{\mu})/2, t/2 + (\bar{\mu} - \underline{\mu})/2]$. The effective tumour is the minimal region that needs to be irradiated to the desired dose level.

With $\tilde{\mu}$ accounted for, let us pose our robust optimization problem as:

$$\begin{aligned} & \underset{m, \gamma}{\text{minimize}} && \gamma(t + 2m) \\ & \text{subject to} && \gamma d_m(y; 0, \tilde{\sigma}) \geq 1, \quad \forall y \in \{\text{effective tumour}\}, \forall \tilde{\sigma} \in [\underline{\sigma}, \bar{\sigma}], \\ & && m, \gamma \geq 0. \end{aligned} \quad (8)$$

Problem (8) appears to have a very similar structure to problem (4). In fact it turns out that they have the *same* structure when suitable adjustments are made for the uncertainty in the mean and standard deviation. In particular, problem (8) is equivalent to

$$\begin{aligned} & \underset{m}{\text{minimize}} && \frac{\bar{t} + 2m}{\Phi\left(\frac{\bar{t}+m}{\bar{\sigma}}\right) - \Phi\left(\frac{-m}{\bar{\sigma}}\right)} \\ & \text{subject to} && m \geq 0, \end{aligned} \quad (9)$$

where $\bar{t} = t + \bar{\mu} - \underline{\mu}$. In other words, if we replace t with $t + \bar{\mu} - \underline{\mu}$ (the size of the effective tumour) and σ with $\bar{\sigma}$ (the maximal standard deviation in its range), all of the results and intuition derived for the “no uncertainty” case hold. To understand how we get formulation (9), consider the dose delivered function accounting for the effective tumour, margin of size m and $\tilde{\sigma}$:

$$d_m(y; 0, \tilde{\sigma}) = \Phi\left(\frac{y + t/2 + m + (\bar{\mu} - \underline{\mu})/2}{\tilde{\sigma}}\right) - \Phi\left(\frac{y - t/2 - m - (\bar{\mu} - \underline{\mu})/2}{\tilde{\sigma}}\right). \quad (10)$$

To determine γ_m^* , we follow the same argument as in Section 2.2. For any $\tilde{\sigma}$, the lowest dose delivered to the effective tumour will occur at its edge. Since larger values of $\tilde{\sigma}$ increase the spread of dose or dose blurring (the function d decreases with increasing $\tilde{\sigma}$), we need to protect against the largest value of $\tilde{\sigma}$, namely, $\bar{\sigma}$. Therefore, plugging $y = t/2 + (\bar{\mu} - \underline{\mu})/2$ and $\tilde{\sigma} = \bar{\sigma}$ into the equation for $d_m(y; 0, \tilde{\sigma})$, setting its reciprocal equal to γ , and replacing γ in the objective function of formulation (8), we arrive at the equivalent formulation (9). Our goal is to derive an optimal margin size (optimal value for m) for any problem instance of the robust problem (a given t , $[\underline{\mu}, \bar{\mu}]$, and $[\underline{\sigma}, \bar{\sigma}]$). Section 3.2 summarizes the results of our analysis.

2.4. Edge-enhanced intensity maps

Edge-enhancements differ from margins in that they provide the flexibility to scale the intensity delivered around the edge of the tumour without modifying the intensity near

the middle of the tumour. We adopt a stylized model of edge-enhancements where the increased intensity delivered at the edge of the tumour is uniform across the increase (a rectangular ‘‘horn’’). An *edge-enhanced intensity map* retains the margin variable m , but adds a variable l that describes the width of the part of the edge-enhancement that extends into the tumour. Finally, there is a variable h that describes the height of the edge-enhancements above the desired dose level. Note the difference between h and γ from the margin intensity map. Variable h is an *additive* amount above the required dose level, whereas γ was a *multiplicative* factor that scales the entire intensity map (for example, $h = 1$ means that the maximum height of the edge-enhanced intensity map is 2, whereas $\gamma = 1$ means that the maximum height of the margin intensity map is 1). Due to the symmetry of the Gaussian distribution, we only consider symmetric intensity maps; however, it would be possible to construct a non-symmetric edge-enhanced intensity map if the motion distribution was skewed in a certain direction (a skewed motion distribution and non-symmetric edge-enhancements were observed in (Chan et al. 2006)). Figure 2 illustrates the relevant variables associated with an edge-enhanced intensity map.

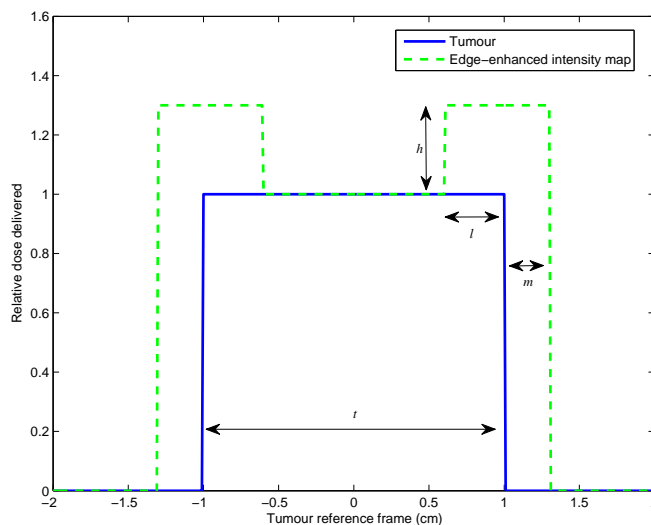


Figure 2. An edge-enhanced intensity map.

As before, we assume that the beam of radiation is centered on the tumour, and both are centered at the origin. We define the static edge-enhanced intensity map, $\delta_{m,l,h}(x)$, to be:

$$\delta_{m,l,h}(x) = \begin{cases} 1, & x \in (-t/2 + l, t/2 - l), \\ 1 + h, & x \in [-t/2 - m, -t/2 + l] \cup [t/2 - l, t/2 + m], \\ 0, & \text{otherwise.} \end{cases} \quad (11)$$

We constrain l to be at most $t/2$, since the two edge-enhancements would overlap if $l > t/2$. Furthermore, note that the special case where $l = t/2$ is exactly the margin

problem from the previous subsection (except for the slight difference in interpretation between h and γ mentioned earlier).

Convolving $\delta_{m,l,h}(x)$ with a Gaussian PDF with mean μ and standard deviation σ , we write the delivered dose $d_{m,l,h}(y; \mu, \sigma)$, as a function of y , as

$$\begin{aligned} d_{m,l,h}(y; \mu, \sigma) = & (1+h)\Phi\left(\frac{y+t/2+m-\mu}{\sigma}\right) - h\Phi\left(\frac{y+t/2-l-\mu}{\sigma}\right) \\ & + h\Phi\left(\frac{y-t/2+l-\mu}{\sigma}\right) - (1+h)\Phi\left(\frac{y-t/2-m-\mu}{\sigma}\right). \end{aligned} \quad (12)$$

The total dose delivered is simply the area under the edge-enhanced intensity map, which is $f(m, l, h) := 2(m+l)(1+h) + t - 2l = t + 2m + 2(m+l)h$. Hence, we can formulate the problem as follows

$$\begin{aligned} & \underset{m,l,h}{\text{minimize}} && t + 2m + 2(m+l)h \\ & \text{subject to} && d_{m,l,h}(y; 0, \sigma) \geq 1, \quad \forall y \in [-t/2, t/2], \\ & && l \leq t/2, \\ & && m, l, h \geq 0. \end{aligned} \quad (13)$$

Similar to how γ^* was written as a function of m in the margin case, the optimal value of h can be written as a function of m and l . This relies on the fact that the edge of the tumour is the most susceptible to being underdosed. The validity of this statement is not obvious; it might seem possible for an edge-enhanced intensity map to ensure sufficient dose to the tumour's edge but not its center. But we can prove that as long as the edge of the tumour receives enough dose, the middle of the tumour is *guaranteed* to also receive enough, for *any* edge-enhanced intensity map. Conversely, if the middle of the tumour is underdosed, then the edge of the tumour will also be underdosed. These statements require a formal proof, which is given in (Chan 2007). After expressing h in terms of m and l , and after simplifying formulation (13), we arrive at

$$\begin{aligned} & \underset{m,l}{\text{minimize}} && f(m, l) \\ & \text{subject to} && m \geq 0, 0 \leq l \leq t/2, \end{aligned} \quad (14)$$

where

$$f(m, l) := t + 2m + 2(m+l) \frac{1 - \Phi\left(\frac{t+m}{\sigma}\right) + \Phi\left(\frac{-m}{\sigma}\right)}{\Phi\left(\frac{t+m}{\sigma}\right) - \Phi\left(\frac{-m}{\sigma}\right) - \Phi\left(\frac{t-l}{\sigma}\right) + \Phi\left(\frac{l}{\sigma}\right)}. \quad (15)$$

As an aside, recall that setting $l = t/2$ recovers the margin problem. We can check this easily by noting that

$$f(m, t/2) = t + \frac{2m(1 - \Phi\left(\frac{t/2}{\sigma}\right) + \Phi\left(\frac{t/2}{\sigma}\right)) + t(1 - \Phi\left(\frac{t+m}{\sigma}\right) + \Phi\left(\frac{-m}{\sigma}\right))}{\Phi\left(\frac{t+m}{\sigma}\right) - \Phi\left(\frac{-m}{\sigma}\right) - \Phi\left(\frac{t/2}{\sigma}\right) + \Phi\left(\frac{t/2}{\sigma}\right)} \quad (16)$$

$$= \frac{t + 2m}{\Phi\left(\frac{t+m}{\sigma}\right) - \Phi\left(\frac{-m}{\sigma}\right)}, \quad (17)$$

which is the same as the objective function in the margin problem.

Our goal is to derive an optimal edge-enhanced intensity map (optimal values for m , l and h) for any problem instance (a given t and σ). In Section 3.3, we will demonstrate our solution to this optimization problem and its implications.

3. Results

The analytical results presented in the upcoming sections were derived by analyzing the structure of the dose deposition functions $f(m)$ (for margins) and $f(m, l)$ (for edge-enhancements). Complete details of the mathematical analyses conducted can be found in (Chan 2007). All computational results were derived using simple function minimization routines in the ‘‘Optimization Toolbox’’ in Matlab.

3.1. Optimal margins

3.1.1. Analytical results For every value of t and σ , there is a unique margin size m^* that minimizes the total dose delivered function $f(m)$. The ratio t/σ is all that is needed to determine the structure of the optimal margin size. If $t/\sigma \leq u^* \approx 2.28$, then the optimal margin size is $m^* = 0$. If $t/\sigma > u^*$, then the optimal margin size is positive, and can be determined by solving a non-linear equation derived from the optimality condition $f'(m) = 0$:

$$2 \left(\int_{-\frac{m}{\sigma}}^{\frac{m+t}{\sigma}} \frac{1}{2\sigma} e^{-\frac{x^2}{2}} dx \right) - \frac{t + 2m}{\sigma\sqrt{2\pi}} \left(e^{-\frac{(m+t)^2}{2\sigma^2}} + e^{-\frac{m^2}{2\sigma^2}} \right) = 0. \quad (18)$$

It is important to note that the threshold u^* is a fundamental constant derived in our analysis and is independent of all the problem parameters. Its exact value is only affected by our assumption that the underlying motion distribution is Gaussian. Different distributions may result in different thresholds.

Figure 3 depicts the relationships between the optimal margin size, corresponding scaling factor, and the tumour size. As the tumour size increases, the optimal margin size increases and the intensity scaling decreases. Adding a larger margin reduces the underdose to the tumour, and therefore, reduces the intensity scaling needed to guarantee tumour coverage. Note that in practical situations where the extent of the motion cannot be arbitrarily large, an optimal solution could involve a positive margin without any intensity scaling ($\gamma_{m^*}^* = 1$). In our framework, this situation appears (approximately) when the standard deviation is much smaller than the size of the tumour, in which case the intensity scaling approaches 1. We provide an example in Appendix B to show that the optimal intensity map may involve a margin with no scaling of the intensity, when the motion PDF is positive only over a bounded domain.

3.1.2. Implications Our structural results establish that if the tumour size is no more than 2.28 times the standard deviation of the motion ($t/\sigma \leq 2.28$), then the optimal margin size is 0. With a margin size of zero, tumour coverage is achieved

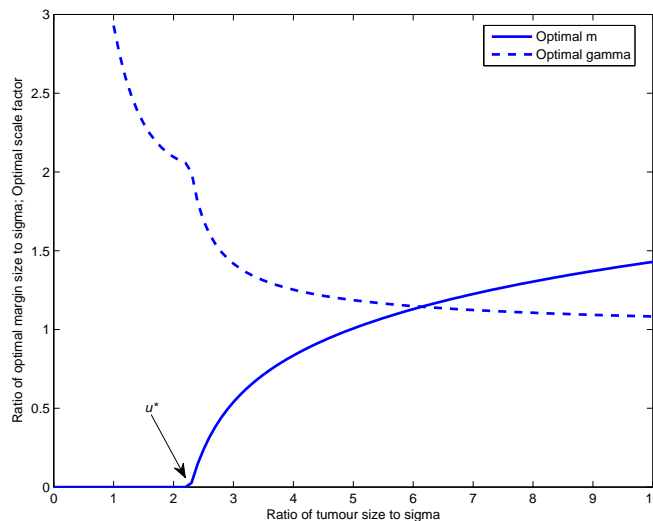


Figure 3. The ratio of the optimal margin size to σ and optimal scale factor as a function of the ratio of the tumour size to σ for a 1D tumour.

purely through a positive scaling of the intensity. This result has a very intuitive interpretation. For small tumours, adding a margin around the tumour is less desirable than simply increasing the intensity of the static intensity map because a margin would be contributing a lot of dose relative to the size of the tumour. If $t/\sigma < 2.28$, then we can think of the tumour as being roughly the same size as the magnitude of the motion, which for realistic amplitudes, implies that the tumour is small. For example, if the standard deviation of the motion amplitude is 0.5 cm, then $t/\sigma < 2.28$ implies that the tumour is roughly 1 cm or smaller. On the other hand, if $t/\sigma > 2.28$, the motion can be thought of as relatively small compared to the size of the tumour, and therefore, adding a small margin around the tumour will only contribute a small increase in the dose delivered to the healthy tissue, relative to the dose delivered to cover the tumour itself. Furthermore, the non-linear equation (18) is easy to solve numerically, which makes computing the optimal margin size straightforward.

3.2. Optimal margins under motion uncertainty

3.2.1. A motivational example We provide motivation by illustrating the negative effects of motion uncertainty when intensity maps are not robust. Consider a tumour spanning the interval $[-1, 1]$, $\tilde{\mu} \in [-1/2, 1/2]$, and $\tilde{\sigma} \in [1/2, 3/2]$. If we ignore or are unaware of the uncertainty and simply assume that $\mu = 0$ and $\sigma = 1$ are fixed, then $t/\sigma = 2 < u^*$ and the optimal intensity map would have $m^* = 0$ and $\gamma_{m^*}^* = (\Phi(2) - \Phi(0))^{-1}$. However, suppose there is a shift in the mean and increased dose blurring during treatment so that the realized mean is at $1/2$ and the realized standard deviation is $3/2$. Then the dose at the edge of the tumour ($y = 3/2$) would be

$$\gamma_{m^*}^* d(y; 1/2, 3/2)|_{y=3/2} \approx 0.856, \quad (19)$$

which corresponds to an underdose of almost 15%. While simplified, this example is meant to convey the importance of accounting for uncertainty in the parameters of the motion distribution. It may be possible to use heuristics to generate robust intensity maps, but we will see an example later on that further argues for the need of a rigorous robust methodology.

3.2.2. Analytical results The uncertainty in the mean and standard deviation change the structure of $f(m)$ slightly, but the general principle described in Section 3.1.1 holds. Instead of using the statistic t/σ , the relevant quantity is $\bar{t}/\bar{\sigma}$, where $\bar{t} = t + \bar{\mu} - \underline{\mu}$. With this modification, the results mirror the “no uncertainty” case. If $\bar{t}/\bar{\sigma} \leq u^*$, then the optimal margin size is 0 and tumour coverage at minimal dose is achieved purely through a positive scaling of the intensity. If $\bar{t}/\bar{\sigma} > u^*$, then the optimal margin size is positive, and can be determined by solving (18), with all instances of t and σ replaced by \bar{t} and $\bar{\sigma}$, respectively. The relationship between the optimal margin size, scaling factor and tumour size is exactly as shown in Figure 3, except with \bar{t} and $\bar{\sigma}$ in place of t and σ , respectively.

3.2.3. Implications These results formalize an underlying relationship between robustness and the type of uncertainty. Loosely speaking, $\tilde{\mu}$ and $\tilde{\sigma}$ are competing with each other to affect the robust solution. Uncertainty in $\tilde{\mu}$ increases the area that requires radiation (effectively increasing the size of the tumour), while the largest possible value of $\tilde{\sigma}$ affects the spread in the realized dose distribution (effectively increasing the minimum dose requirement). Thus, it seems like a margin is an appropriate compensatory tool for dealing with uncertainty in $\tilde{\mu}$, while increasing the intensity of the beam can offset an increased $\tilde{\sigma}$. The relationship between the ratio $\bar{t}/\bar{\sigma}$ and $u^* \approx 2.28$ solidifies this intuition. If the uncertainty in $\tilde{\mu}$ is large, then \bar{t} will be large, and it is more likely that the optimal robust solution will consist of a positive margin (i.e., when $\bar{t}/\bar{\sigma} > u^*$). On the other hand, if $\bar{\sigma}$ is large, then it is more likely that the optimal robust solution will be a pure intensity scaling with no positive margin (i.e., when $\bar{t}/\bar{\sigma} < u^*$). Our intuition here is similar to that from the nominal (no uncertainty) case, but now we are incorporating uncertainty in $\tilde{\mu}$ and the largest value of $\tilde{\sigma}$ into the ratio.

3.2.4. A robust example We close this section by demonstrating that the optimal robust solution from formulation (9) provides better dose minimization than a particular, intuitive heuristic procedure. In principle, one way to generate a robust solution would be to solve the nominal (no uncertainty) problem (4) for every realization of $\tilde{\mu}$ and $\tilde{\sigma}$, and then take the “union” of the resulting solutions. A robust solution generated from this method would be the smallest intensity map that contains the intensity maps corresponding to the solution of the nominal problem (4) for every realization of $\tilde{\mu}$ and $\tilde{\sigma}$. While this method produces an intensity map that ensures tumour coverage, this intensity map will deliver more total dose than is necessary, as we show next.

Let $t = 2$, $\tilde{\mu} \in [-1/2, 1/2]$ and $\tilde{\sigma} = \sigma = 1$ (no uncertainty in σ for simplicity). Since $t/\sigma < u^*$, the solution to problem (4) will be a pure intensity scaling, whereas the robust solution will involve a positive margin (since $\bar{t}/\sigma = 3 > u^*$). Solving the robust problem (9) with $\bar{t} = 3$ results in a robust solution, $R1$, with a margin of size $m_{R1}^* = 0.539$, and an intensity scaling factor of 1.418. Thus, the total dose delivered by the robust solution, $R1$, is $\gamma_{m^*}^*(\bar{t} + 2m^*) = 1.418(3 + 2 \cdot 0.539) = 5.785$.

The optimal solution for the nominal problem is $m_N^* = 0$ with an intensity scaling factor of 2.095. The heuristic robust intensity map, $R2$, generated from these nominal solutions is

$$\delta_{R2}(y) = \begin{cases} 2.095, & y \in [-t/2 + \underline{\mu} - m_N^*, t/2 + \bar{\mu} + m_N^*] = [-1.5, 1.5], \\ 0, & \text{otherwise,} \end{cases} \quad (20)$$

which leads to a total delivered dose of $2 \cdot 1.5 \cdot 2.095 = 6.286$ – roughly a 9% increase in total dose delivered as compared to the robust solution $R1$.

In this example, while t is small relative to σ , the uncertainty in $\tilde{\mu}$ forces the effective tumour size over the threshold u^* (i.e., $\bar{t} > u^* > t$). Thus, the heuristic robust intensity map (i.e., union of nominal intensity maps) is a union of purely scaled intensity maps, whereas the optimal robust intensity map involves a positive margin with a smaller scaling factor. The example shows that there can be relatively significant gains in terms of dose minimization by using the optimal robust solution from an appropriately formulated mathematical problem (formulation (9)), as opposed to generating a robust solution using a heuristic procedure involving only solutions of the no-uncertainty version of the problem.

3.3. Optimal edge-enhancements

3.3.1. Analytical results As in the margin problem, we discovered that the optimal edge-enhanced intensity map structure bifurcates into two cases, based on the ratio t/σ and its relationship to a constant $\hat{u} \approx 2.11$. If $t/\sigma \leq \hat{u}$, then $m^* = 0$ and $l^* = t/2$. In other words, the optimal solution involves a positive intensity scaling with no margin or edge-enhancements. If $t/\sigma > \hat{u}$, then the optimal solution has edge-enhancements but no margin: $m^* = 0$ and $l^* \in (0, t/2)$. In this case, l^* can be determined by solving a non-linear equation derived from the optimality condition $\partial f(m, l)/\partial l = 0$, with $m = 0$:

$$\int_0^{\frac{t}{\sigma}} \frac{1}{\sqrt{2\pi}} e^{-\frac{x^2}{2}} dx - \int_{\frac{l}{\sigma}}^{\frac{t-l}{\sigma}} \frac{1}{\sqrt{2\pi}} e^{-\frac{x^2}{2}} dx - \frac{l}{\sigma\sqrt{2\pi}} \left(e^{-\frac{(t-l)^2}{2\sigma^2}} + e^{-\frac{l^2}{2\sigma^2}} \right) = 0. \quad (21)$$

Figures 4(a) and 4(b) show l^*/σ and h^* as a function of t/σ , respectively. Figure 4(a) shows that l/σ scales linearly with t/σ with slope 1/2 (i.e., $l^* = t/2$ and no edge-enhancements) until \hat{u} , at which point $l^* < t/2$ and edge-enhancements emerge. It appears that l^*/σ is quite sensitive to t/σ ; indeed, l^*/σ decreases quickly for small increases in t/σ beyond \hat{u} . Figure 4(b) shows the corresponding edge-enhancement height h^* , which is the minimum height necessary to bring the dose at the edge of the tumour up to the requirement. Initially, as t/σ grows, the tumour edge underdosage

shrinks (think of the Gaussian as being convolved with a square wave that is becoming wider), so h^* follows suit. But when the ratio moves into the edge-enhancement region, l^* shrinks, so h^* needs to grow in order to maintain tumour coverage at the tumour edge.

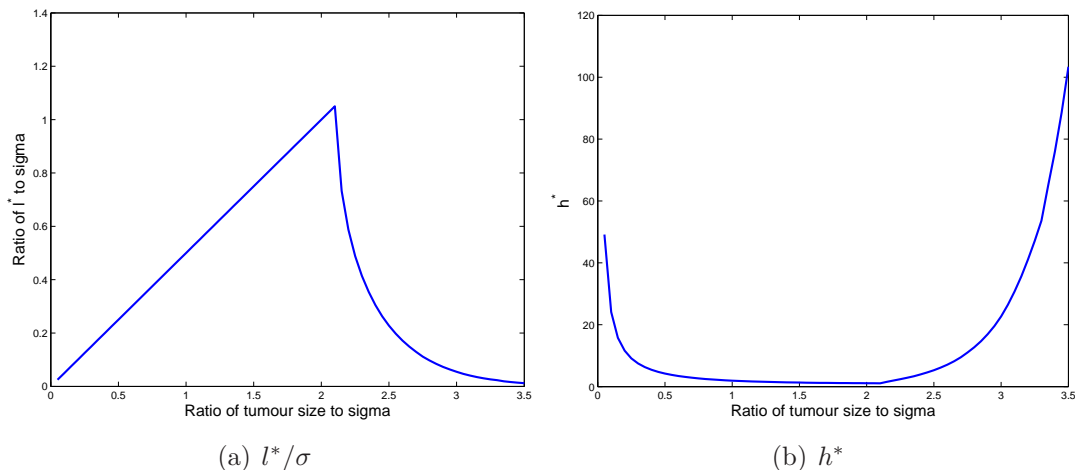


Figure 4. Optimal parameters of an edge-enhanced intensity map as a function of the ratio of the tumour size to σ for a 1D tumour.

3.3.2. Implications Intuitively, we should not be surprised that $\hat{u} < u^*$. Since edge-enhancements are a generalization of margins (recall that the margin analysis is a special case of the edge-enhancement analysis when $l = t/2$), we would expect the threshold for when edge-enhancements are optimal to be lower (in other words, satisfied by more possible values of t/σ) than the corresponding one for margins.

Our results imply that either edge-enhancements or pure intensity scalings demonstrate improved dose minimization over margins for any ratio t/σ . Furthermore, when the optimal intensity map is edge-enhanced, the result that $m^* = 0$ suggests that the edge-enhancements should only be present inside the tumour and not expand into the region surrounding the tumour. By allowing the flexibility of creating edge-enhanced intensity maps, a margin will never be preferred, and instead edge-enhancements will be used if t/σ is sufficient large. However, realistically deliverable intensity maps will not permit arbitrarily thin and high edge-enhancements (which Figure 4(b) suggests is optimal when t becomes large), so at some physical limit (which could be included into the optimization problem (14) as a lower bound on l), margins will be used in conjunction with edge-enhancements in order to create an optimal intensity map (i.e., both $m^* > 0$ and $0 < l^* < t/2$).

4. Discussion and conclusions

In this paper, we presented a new methodological approach for determining margin and edge-enhanced intensity maps that guarantee delivery of a minimally-sufficient amount of dose to a tumour in the presence of Gaussian motion and motion uncertainty. We believe our results can be used to guide treatment planning decisions by providing rules of thumb or recipes for intensity map design.

In the case of margins, we found that if the ratio of the tumour size to the standard deviation of motion is less than 2.28, then the optimal intensity map involves no margins and is simply a pure scaling increase of the static intensity map to compensate for the dose blurring created by motion. On the other hand, if the tumour is at least 2.28 times the size of the standard deviation of motion, then an isotropic margin around the tumour (along with an intensity scaling) is optimal in terms of providing tumour coverage at minimal dose. For the latter, we derived a non-linear equation that when solved, provides the optimal size of the margins. We also derived a formula that produces the optimal scaling factor using the optimal margin size. These results buttress the intuition that for small tumours (e.g., less than 1 cm in length/diameter), margins need not be used and a pure intensity scaling can be enough to compensate for the dose blurring due to motion (e.g., $\sigma \approx 0.5$ cm).

We provided the first “robust” analysis of margin intensity maps in the presence of motion uncertainty. We noted that the presence of motion itself is not necessarily a source of uncertainty, but that uncertainty in the parameters (e.g., the mean and standard deviation) of the motion distribution imply motion uncertainty. In this case, we showed that the robust margin problem had the same structure as the nominal margin problem, and therefore the 2.28 threshold remained valid when examining a modified ratio of the effective tumour size divided by the maximum standard deviation. By adding the magnitude of the uncertain range for the mean to the tumour size and dividing the sum by the maximum value in the uncertain range for the standard deviation, this ratio could be used to determine whether or not the optimal robust margin intensity map had a positive margin or was a pure intensity scaling.

Finally, in the case of edge-enhancements, we found that if the ratio of the tumour size to standard deviation of motion is less than 2.11, then again the optimal intensity map is a pure scaling increase of the intensity. When this ratio is larger than 2.11, edge-enhancements are optimal and we derived equations that generate the optimal values of their height and width. Given the added flexibility that edge-enhancements afford over margins, we found that edge-enhancements or pure intensity scalings will always be preferred over margins, though realistically deliverable intensity maps may involve a combination of edge-enhancements and margins. Edge-enhanced intensity maps could be realized in practice using, for example, additional MLC apertures focused on the tumour edge, which would be designed via optimization.

Logical extensions of the work presented in this paper include extending the robust analysis to edge-enhanced intensity maps. Initial analytical and computational results

are presented in (Chan 2007), but there is an opportunity for further exploration, especially in the area of robust edge-enhancements. Extensions to higher dimensions should be explored as well. We have extended the margin analysis to three dimensions in Appendix C, but the extension to 3D edge-enhancements is fertile ground for further research. Finally, explicit consideration of the type of neighbouring healthy tissue is important. We used an objective of minimizing total dose, which is appropriate when considering neighbouring parallel organs. Organs that are sensitive to the maximum dose delivered (e.g., the spinal cord) would need to be analyzed differently.

Acknowledgments

This research was supported in part by the Hugh Hampton Young Memorial Fund fellowship, the Natural Sciences and Engineering Research Council of Canada, Siemens Corporate Research, Inc., and the National Cancer Institute under grant R01-CA103904 and grant R01-CA118200.

Appendix A. Derivation of the structure of the objective function $f(m)$ in Section 3.1

In this section, we give a flavour of the mathematical arguments used to justify the results in this paper. As noted previously, all omitted proofs are provided in (Chan 2007). As an example, we focus on the derivation of the structure of $f(m)$ and the subsequent results involving t/σ and u^* . Recall that

$$f(m) := \frac{t + 2m}{\Phi\left(\frac{t+m}{\sigma}\right) - \Phi\left(\frac{-m}{\sigma}\right)}. \quad (\text{A.1})$$

We can show that either:

- (i) $f(m)$ has a unique minimum at some $m^* > 0$, or
- (ii) $f(m)$ has a unique minimum at $m^* = 0$.

Let us define $g(m)$ to be the denominator in the definition of $f(m)$. Since $g(m)$ equals a certain area under the curve of the standard normal (Gaussian) probability density function, it is strictly positive for $m \geq 0$. By taking derivatives, it is easy to show that $g'(m) > 0$ and $g''(m) < 0$ for $m \geq 0$. Next, we consider the first two derivatives of $f(m)$:

$$f'(m) = \frac{2g(m) - (t + 2m)g'(m)}{g^2(m)} \quad (\text{A.2})$$

and

$$f''(m) = \frac{-(t + 2m)g''(m)g^2(m) - (2g(m) - (t + 2m)g'(m))2g(m)g'(m)}{g^4(m)}. \quad (\text{A.3})$$

Note that $f(m)$ is continuous and differentiable. Also, $f(m) > 0$ for all $m \geq 0$, and in particular, $\lim_{m \rightarrow \infty} f(m) = \infty$. The two cases for the structure of $f(m)$ are obtained depending on whether or not $f'(m)$ has a positive root.

If there is an $m^* > 0$ that satisfies $f'(m^*) = 0$, then m^* must be a strict local minimum because we have $g''(m) < 0$ and

$$f''(m^*) = \frac{-(t + 2m^*)g''(m^*)}{g^2(m^*)} > 0. \quad (\text{A.4})$$

Furthermore, such an m^* is unique. To see why, consider the existence of another $\hat{m} > 0$ that satisfies $f'(\hat{m}) = 0$. This \hat{m} must be a strict local minimum as well, but between two strict local minimum there must be a strict local maximum due to the Intermediate Value Theorem (with continuity of $f'(m)$), which contradicts the fact that all stationary points of $f(m)$ are strict local minima. This covers the first possibility of the structure of $f(m)$.

On the other hand, if there is no $m > 0$ such that $f'(m) = 0$, then we claim $f'(m) > 0$ for all $m > 0$. Suppose to the contrary that there exists $\hat{m} > 0$ such that $f'(\hat{m}) < 0$. Since $f'(m) \rightarrow 2 > 0$ as $m \rightarrow \infty$, $f'(m)$ must cross 0 at some point, implying the existence of a solution to $f'(m) = 0$ on (\hat{m}, ∞) , which is a contradiction. Since $f(m)$ is increasing, it must be minimized at $m = 0$. This covers the second case.

Since $f(m) \rightarrow \infty$ as $m \rightarrow \infty$, the first case is equivalent to $f'(0) < 0$ and the second case is equivalent to $f'(0) \geq 0$. There is, therefore, a threshold that is crossed if $f'(0) = 0$. If we substitute $m = 0$ into the numerator of the equation for $f'(m)$, and substitute $u = t/\sigma$ into the subsequent equation, we get

$$h(u) := \left(\int_{-u}^u \frac{1}{\sqrt{2\pi}} e^{-\frac{x^2}{2}} dx \right) - \frac{u}{\sqrt{2\pi}} \left(1 + e^{-\frac{u^2}{2}} \right) = 0. \quad (\text{A.5})$$

From here, it is straightforward to show that $u^* \approx 2.28$ is the only positive solution to this equation (a simple plot suffices), and is a threshold that separates $h(u) > 0$ (for $0 < u < u^*$) from $h(u) < 0$ (for $u > u^*$).

Appendix B. Example of an optimal margin intensity map with no intensity scaling

Consider a tumour centered at the origin, occupying the interval $[-1, 1]$. If the motion PDF is

$$p(x) = \begin{cases} 1, & x \in [-1/2, 1/2], \\ 0, & \text{otherwise,} \end{cases} \quad (\text{B.1})$$

and the static intensity map is

$$\delta_m(x) = \begin{cases} 1, & x \in [-1 - m, 1 + m], \\ 0, & \text{otherwise,} \end{cases} \quad (\text{B.2})$$

then the dose delivered as a function of the location, y , is

$$d_m(y) := \int_{-\infty}^{\infty} \delta_m(y - x)p(x)dx \quad (\text{B.3})$$

$$= \int_{\max\{y-1-m, -1/2\}}^{\min\{y+1+m, 1/2\}} 1 dx \quad (\text{B.4})$$

$$= \begin{cases} y + 3/2 + m, & \text{if } y \leq -1/2 - m, \\ 1, & \text{if } -1/2 - m \leq y \leq 1/2 + m, \\ 3/2 + m - y, & \text{if } y \geq 1/2 + m. \end{cases} \quad (\text{B.5})$$

Note that we may restrict m to be between 0 and $1/2$ since we can achieve tumour coverage with any margin of size at least $1/2$ (and no intensity scaling). The minimum of $d_m(y)$ over $y \in [-1, 1]$ occurs at $y = \pm 1$, and at those points, $d_m(-1) = d_m(1) = 1/2 + m$. Hence, the minimal intensity scaling factor is

$$\gamma_m^* = \frac{1}{1/2 + m} \quad (\text{B.6})$$

and the total dose delivered is

$$f(m) := \frac{2 + 2m}{1/2 + m}. \quad (\text{B.7})$$

The derivative of $f(m)$,

$$f'(m) = \frac{-1}{(1/2 + m)^2}, \quad (\text{B.8})$$

is negative for all $m \geq 0$. Thus, the optimal solution is to have a positive margin of size $1/2$, and then no intensity scaling is needed.

Appendix C. Analysis of 3D margins

In this section, we provide an overview of the margin analysis extension to three dimensions. A full analysis is available in (Chan 2007). In three dimensions, we consider a spherical tumour moving according to a 1D Gaussian. We define a *3D margin* as an expansion of the spherical static intensity map in the direction of motion, as shown in Figure C1.

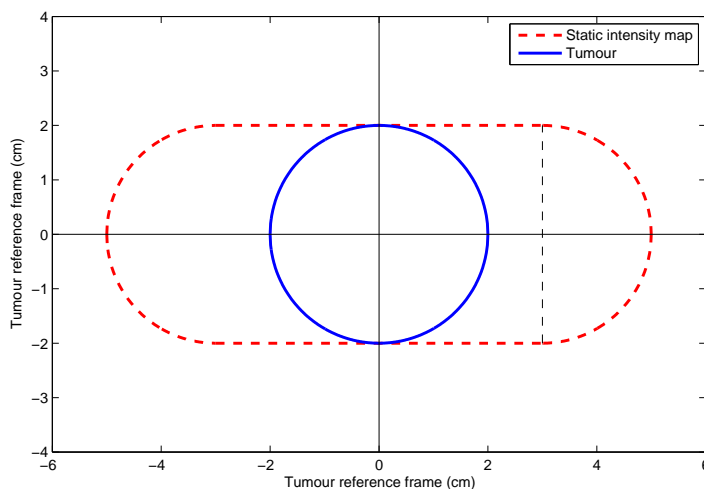


Figure C1. A two-dimensional slice of the three-dimensional static intensity map.

Appendix C.1. Optimal 3D margins

With a spherical tumour in the presence of Gaussian motion, we observed that there were points on the surface of the tumour that would receive no dose at all if no margin was applied. The intuition is that the equatorial ring of points perpendicular to the direction of motion do not receive dose from neighbouring parts of the static intensity map during convolution. Therefore, we showed that a margin was always needed to guarantee tumour coverage. The margin expanded the static intensity map in the direction of motion, ensuring that the ring of points would receive a positive amount of radiation after convolution. We derived a formula to calculate the exact margin size as a function of t and σ .

Appendix C.2. Optimal 3D margins under motion uncertainty

Uncertainty in the Gaussian parameters resulted in a problem that was similar in structure to the 1D version. Due to the uncertainty in the mean, the effective tumour was no longer spherical, but elongated in the direction of motion. Therefore, the problematic ring of points from the “no uncertainty” case disappeared, and the optimal 3D margin intensity map had either a positive or zero margin, depending on the values of t and σ . We derived a complex series of thresholds that determines whether a positive margin or no margin is optimal. We also derived a general rule of thumb stating that if the effective tumour was long and skinny (its length at least ~ 8 times its width), then it was possible for the optimal 3D margin size to be zero. Otherwise, the optimal 3D margin would always be positive.

References

- Balter J M, Sandler H M, Lam K, Bree R L, Lichter A S and ten Haken R K 1995 Measurement of prostate movement over the course of routine radiotherapy using implanted markers *Int. J. Radiat. Oncol. Biol. Phys.* **31**, 113–118.
- Bertsekas D P and Tsitsiklis J N 2002 *Introduction to Probability* Athena Scientific Belmont, Massachusetts.
- Biggs P J and Shipley W U 1986 A beam width improving device for a 25 MV x ray beam *Int. J. Radiat. Oncol. Biol. Phys.* **12**, 131–135.
- Bortfeld T, Chan T C Y, Trofimov A and Tsitsiklis J N 2008 Robust Management of Motion Uncertainty in Intensity-Modulated Radiation Therapy *Oper. Res.* **56**(6), 1461–1473.
- Bortfeld T, Jiang S B and Rietzel E 2004 Effects of motion on the total dose distribution *Semin. Radiat. Oncol.* **14**(1), 41–51.
- Bortfeld T, Jokivarsi K, Goitein M, Kung J and Jiang S B 2002 Effects of intra-fraction motion on IMRT dose delivery: statistical analysis and simulation *Phys. Med. Biol.* **47**(13), 2203–2220.
- Brugmans M J, van der Horst A, Lebesque J V, and Mijnheer B J 1999 Beam intensity modulation to reduce the field sizes for conformal irradiation of lung tumors. a dosimetric study *Int. J. Radiat. Oncol. Biol. Phys.* **43**, 893–904.
- Chan T C Y 2007 Optimization under Uncertainty in Radiation Therapy PhD thesis Massachusetts Institute of Technology.
- Chan T C Y, Bortfeld T and Tsitsiklis J N 2006 A robust approach to IMRT optimization *Phys. Med. Biol.* **51**(10), 2567–2583.

- Dirkx M L, Heijmen B J, Korevaar G A, van Os M J, Stroom J C, Koper P C and Levendag P C 1997 Field margin reduction using intensity-modulated x-ray beams formed with a multileaf collimator *Int. J. Radiat. Oncol. Biol. Phys.* **38**, 1123–1129.
- Ekberg L, Holmberg O, Wittgren L, Bjelkengren G and Landberg T 1998 What margins should be added to the clinical target volume in radiotherapy treatment planning for lung cancer? *Radiother. Oncol.* **48**, 71–78.
- Engelsman M, Sharp G C, Bortfeld T, Onimaru R and Shirato H 2005 How much margin reduction is possible through gating or breath hold? *Phys. Med. Biol.* **50**, 477–490.
- Goitein M 1985 Calculation of the uncertainty in the dose delivered during radiation therapy *Med. Phys.* **12**, 608–612.
- Goitein M 2004 Organ and tumor motion: an overview *Semin. Radiat. Oncol.* **14**(1), 2–9.
- International Commission on Radiation Units and Measurements 1999 *ICRU report 62: Prescribing, recording and reporting photon beam therapy* ICRU Bethesda.
- Lind B K, Kallman P, Sundelin B and Brahme A 1993 Optimal radiation beam profiles considering uncertainties in beam patient alignment *Acta Oncol.* **32**, 331–342.
- Lof J, Lind B K and Brahme A 1995 Optimal radiation beam profiles considering the stochastic process of patient positioning in fractionated radiation therapy *Inverse Problems* **11**(6), 1189–1209.
- Lujan A E, Larsen E W, Balter J M and Ten Haken R K 1999 A method for incorporating organ motion due to breathing into 3D dose calculations *Med. Phys.* **26**(5), 715–720.
- Mohan R, Wu Q, Wang X and Stein J 1996 Intensity modulation optimization, lateral transport of radiation, and margins *Medical Physics* **23**(12), 2011–2021.
- Roach M, Pickett B, Rosenthal S A, Verhey L and Phillips T L 1994 Defining treatment margins for six field conformal irradiation of localized prostate cancer *Int. J. Radiat. Oncol. Biol. Phys.* **28**, 267–275.
- Schewe J E, Balter J M, Kwok L L and Haken R K T 1996 Measurement of patient setup errors using port films and a computer-aided graphical alignment tool *Med. Dosim.* **21**, 97–104.
- Sharpe M B, Miller B M and Wong J W 2000 Compensation of x-ray beam penumbra in conformal radiotherapy *Medical Physics* **27**(8), 1739–1745.
- Sheng K, Cai J, Brookeman J, Molloy J, Christopher J and Read P 2006 A computer simulated phantom study of tomotherapy dose optimization based on probability density functions (pdf) and potential errors caused by low reproducibility of pdf *Med. Phys.* **33**(9), 3321–3326.
- Sir M Y, Pollock S M, Epelman M A, Lam K L and Haken R K T 2006 Ideal spatial radiotherapy dose distributions subject to positional uncertainties *Phys. Med. Biol.* **51**, 6329–6347.
- Thomas S J 1994 Factors affecting penumbral shape and 3D dose distributions in stereotactic radiotherapy *Phys. Med. Biol.* **39**, 761–771.
- Trofimov A, Rietzel E, Lu H M, Martin B, Jiang S, Chen G T Y and Bortfeld T 2005 Temporo-spatial IMRT optimization: concepts, implementation and initial results *Phys. Med. Biol.* **50**(12), 2779–2798.
- Ulmer W and Harder D 1995 A triple gaussian pencil beam model for photon beam treatment planning *Z. Med. Phys.* **5**, 25–30.
- Unkelbach J and Oelfke U 2004 Inclusion of organ movements in IMRT treatment planning via inverse planning based on probability distributions *Phys. Med. Biol.* **49**(17), 4005–4029.
- van Herk M, Remeijer P, Rasch C and Lebesque J V 2000 The probability of correct target dosage: dose-population histograms for deriving treatment margins in radiotherapy *Int. J. Radiat. Oncol. Biol. Phys.* **47**(4), 1121–1135.
- Webb S 2006 Motion effects in (intensity modulated) radiation therapy: a review *Phys. Med. Biol.* **51**, R403–R425.
- Zhang T, Jeraj R, Keller H, Lu W, Olivera G H, McNutt T, Mackie T and Paliwal B 2004 Treatment plan optimization incorporating respiratory motion *Med. Phys.* **31**(6), 1576–1586.